encit 2020

ABCM Associação Brasileira de Engenharia e Ciências Mecânicas

18th Brazilian Congress of Thermal Sciences and Engineering
November 16-20, 2020, Bento Gonçalves, RS, Brazil

ENC-2020-0237
THERMOECONOMIC ASSESSMENT OF HYBRID-ELECTRIC PROPULSION FOR AIRCRAFTS

Gabriel Siqueira Machado, gabriel.machado@mecanica.coppe.ufrj.br[1]
Yipsy Roque Benito, yipsy.benito@engenharia.ufjf.br[2]
Manuel A. Rendón, manuel.rendon@ufjf.edu.br[2]
Monica Carvalho, monica@cear.ufpb.br [3]
Pablo Roque Diaz, roquediazpablo@gmail.com[4]

[1]Alberto Luiz Coimbra Institute of Graduate Studies and Engineering Research - COPPE - Department of Mechanical Engineering, Federal University of Rio de Janeiro - UFRJ, Rio de Janeiro, Brazil.

[2] Federal University of Juiz de Fora - UFJF, Campus Universitário, Rua José Lourenço Kelmer, s/n - São Pedro, Juiz de Fora - MG, 36036-900

[3] Department of Renewable Energy Engineering, Federal University of Paraíba - UFPB, João Pessoa, Paraíba, Brazil.

[4] Centro de Estudios de Energía y Tecnologías Ambientales, Universidad Central Marta Abreu de Las Villas, Cuba

Abstract: *This study develops the thermoeconomic assessment of a hybrid-electric propulsion system for aircrafts. A mathematical model was built to describe the behavior of all components of the system, and the Theory of Exergy Cost was applied to determine the variation of the global exergy efficiency and exergy costs of power with respect to the degree of hybridization of the aircraft. The points with highest efficiency and lowest costs were identified.*

Keywords: *Hybridization degree; Exergoeconomics; Exergy cost; Exergy efficiency; Computational simulation.*

1. INTRODUCTION

With the technological advances and increase in global energy demands, new energy conversion pathways have been developed and perfected throughout the years. One of the alternatives to improve the performance is hybrid-electric propulsion (Friedrich & Robertson, 2015), which combines two different energy resources and takes advantage of their individual benefits. An overview of the challenges and potential benefits associated with the design of aircrafts that use hybrid-electric propulsion systems was presented by Finger et al. (2018), who emphasized that the applicability ranges from small unmanned aerial vehicles to man-carrying aircraft. Other issues regarding battery technology and other propulsion system elements and technologies were highlighted by Sziroczak et al. (2020).

Due to the inherent complexity of combining two different energy resources, energy management is vital to organize the available resources. Besides affecting the costs associated with energy resources, hybrid propulsion can minimize space and deadweight load requirements and redirect exergy reserves to the different phases of flight, enabling the rationalization of the flight mission plan regarding payload, execution time, and other qualitative indicators. Indicators of the specific energy of the battery and exergy content of the fuel are critical. One of the most important parameters related to energy management in a hybrid vehicle is the degree of hybridization, ϕ, which is the ratio of the output power from an energy source to the total output power of the powertrain (Song et al., 2019). Complete energy management must also include the characterization of all energy and exergy flows of the system, instant power requirements, translation speed, total energy, duration and availability of payload for the different phases of the flight mission. From a purely thermoeconomic viewpoint, the allocation of costs to these flows is an important decision factor, along with the administration

of every energy source involved, including land preparation costs, such as fuel logistics and battery charge. Different propulsion operation strategies were tested by Hoelden et al. (2018) for hybrid-electric aircrafts powered by conventional gas turbines and battery-powered electric motors, who underlined the importance of selecting a suitable power-to-energy-ratio of the battery according to the flight mission.

From an exergy point of view, the global exergy efficiency is the relationship between the exergy of products and fuels, being a measure of the thermodynamic perfection of systems and processes. For the calculation of exergy-based efficiencies, the thermodynamic conditions of the environment and of any pre-established control volumes must be taken into account. Gandolfi et al. (2010) already highlighted the applicability of exergy analysis as a decision making tool for aircraft system design and optimization, and Koruyucu (2019) developed exergy analyses for different ϕ for a hybrid electric propulsion light utility helicopter engine.

From an economic viewpoint, the definitions of the Theory of Exergy Cost (TEC) (Lozano and Valero, 1993) can be employed. TEC presents a series of postulates with the objective of building a system of equations to determine the exergy costs of the internal flows and products of a system. Each equation represents a subsystem and each flow represents the amount of exergy consumed to obtain the flow. Exergy and thermoeconomics were employed by Affonso et al. (2019) to compare conventional and hybrid electric propulsion systems for a regional aircraft. The authors also presented a literature review on the application of exergy assessments in the aerospace industry, and demonstrated that an integrated exergo-economic analysis enables the evaluation of the global exergy efficiency when operating in a specific country or region (the unit cost of exergy generation is very site-dependent). These authors have also highlighted the importance of other specific performance indicators based on exergy cost indices for the exergy content of products, but also associated with thrust, extra power requirements for takeoff (and specific phases of the flight), and the possibilities of optimizing space and payload capacity.

With the combination of two different energy sources, new challenges arise such as an increase in the complexity of the design, construction, maintenance and energy management. Therefore it is necessary to count with a reliable model that predicts the behavior of each equipment and its dynamics with global exergy efficiency, making the best use of the existing exergy reserves onboard at the beginning of the mission.

The overarching aim of this study is to carry out a thermoeconomic assessment of a hybrid-electric propulsion system for aircrafts, and study the influence of the ϕ on the unit exergy costs of the final product (exergy output at the propeller). This study models the effect of ϕ, expressed by the average and instantaneous electrochemical (battery charge exergy) and thermochemical (fuel exergy) exergy fractions, on the total and instantaneous exergy consumption coefficients. To this end, the hybrid-electric system was modelled on a test bench for aeronautical propulsion, and its energy and exergy behaviors were simulated at fixed (nominal) power and variable ϕ. An thermoeconomic study can minimize the costs of energy (exergy) resources, making the best use of available space and payload. To this end, it is necessary to comprehend the internal relationships between the different exergy flows in the hybrid scheme, which is precisely the starting point of this study.

2. MATERIALS AND METHODS

The study object is a test bench for hybrid-electric propulsion, for application in light aircrafts, which is part of a wider research project carried out by the Electromechanical Energy Conversion Group at the Federal University of Juiz de Fora (Southeast Brazil). The study object consists of an electric-driven propeller, driven by an AC electric motor, which can be powered by a combined system - gas turbine (fossil fuel) and a battery bank. A detailed description is presented by Machado (2019).

The electric motor can be powered by both sources, employing a converter that enables different combinations of power and rpm through the regulation of frequency and tension. The exergy reserve for each test that simulates the specific requirements of a flight program or mission is defined by the mass of fuel initially in the tank and the initial charge level of the battery (given by its initial tension). The results of the tests provide several performance indicators of the propeller, such as instant mechanical power measurements at the electric motor, rotation speed, flow speed regarding still air, fuel consumption rates, properties of exhaust gases of the turbine, and dynamics of the fuel tank level and charge status of the battery. All these measurements provide data on the supply and management of exergy to the aircraft and efficiency of conversion into a useful product to the mission. These *useful products* are the mechanical power for the movement of the aircraft and its safe operation during takeoff, landing, and cruising regimen.

Figure 1 shows the bench test, which includes the fuel tank (STG), gas turbine + driven electrical generator (ICE), converters (CON), batteries (BAT), electrical engine (EME) and propeller (PRP) in a serial-hybrid configuration (Figure 2).

Figure 1. Bench test for hybrid-electric propulsion

Figure 2 shows the main energy flows that connect the components of the system. The losses are represented by L, power is represented by W, and η represents the efficiencies. The fuel tank provides energy to the internal combustion engine, which is connected to the converters along with a battery that drives the electric engine, which transmits the power required to move the propeller.

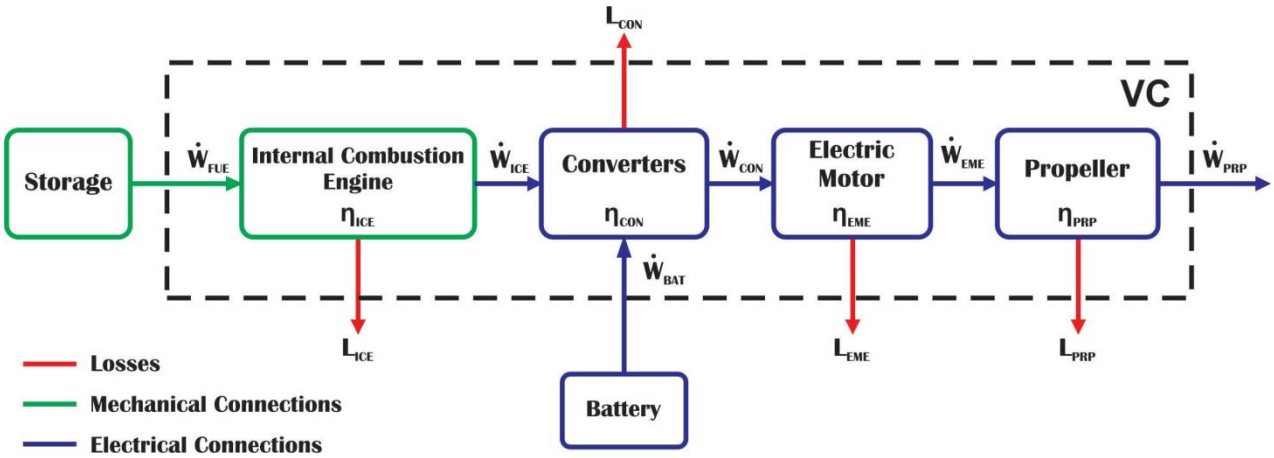

Figure 2. Physical structure of the hybrid-electric propulsion system

The hybrid system can operate in two different ways: i) battery providing power to the converters, in discharging mode, and ii) battery receiving energy, in charging mode. This study focuses on the former. The main focus of the study is to analyze parameters such as power, efficiency, and cost of each component in relation to the variation of ϕ. Variations in missions and flight time are important because during takeoff, the power of components is maximal, which is not the case during cruising and landing - herein a single flight plan is considered.

2.1. Thermodynamic model

The thermodynamic model considered the following simplifying assumptions: i) there is no energy dissipation in the fuel tank or battery; ii) the battery presents constant specific energy; iii) Steady-state conditions were considered for ICE, CON, EME, and PRP; iv) variations of potential energy were not considered, and v) operation of the battery followed nominal conditions (see section 2.2).

The ϕ, as defined by Buecherl et al (2009), is an adimensional coefficient (ϕ) that compares the amount of electric power originating from the battery ($\dot{W}_{BAT}$) with the total power $\dot{W}_{ICE} + \dot{W}_{BAT}$, as shown in Eq (1).

$$\phi = \frac{\dot{W}_{BAT}}{\dot{W}_{BAT} + \dot{W}_{ICE}} \quad (1)$$

ϕ is zero when the aircraft operates with conventional propulsion (ICE only) and therefore $\dot{W}_{BAT} = 0$. When $\phi = 1$, the aircraft operates with electric propulsion only ($\dot{W}_{ICE} = 0$). From the physical structure shown in Figure 2, energy balances are developed for the control volumes. The rates of fuel energy entering the ICE ($\dot{W}_{FUE}$) and exiting the batteries ($\dot{W}_{BAT}$) were considered constant and utilized in all equations. The rate of energy entering the ICE is expressed by Eq. (2).

$$\dot{W}_{ICE} = \dot{W}_{FUE} \cdot \eta_{ICE} \quad (2)$$

η represents the efficiencies. The outlet power of the converters ($\dot{W}_{CON}$) is given by Eq. (3).

$$\dot{W}_{CON} = \dot{W}_{ICE} \cdot \eta_{CON;1} + \dot{W}_{BAT} \cdot \eta_{CON;2} \quad (3)$$

The power of the electrical engine ($\dot{W}_{EME}$) and of the propeller ($\dot{W}_{PRP}$) are given by Eq. (4) and (5), respectively.

$$\dot{W}_{EME} = \dot{W}_{CON} \cdot \eta_{EME} \quad (4)$$

$$\dot{W}_{PRP} = \dot{W}_{EME} \cdot \eta_{PRP} \quad (5)$$

2.2. Energy and exergy assessments

This study analyzes a system that counts with two different energy sources. Emptying the fuel tank directly affects the final weight of the aircraft. Discharging the battery affects its tension, causing a lower nominal power. Details on these sources are presented next. The discharge curve of the battery with time is shown in Fig. (3).

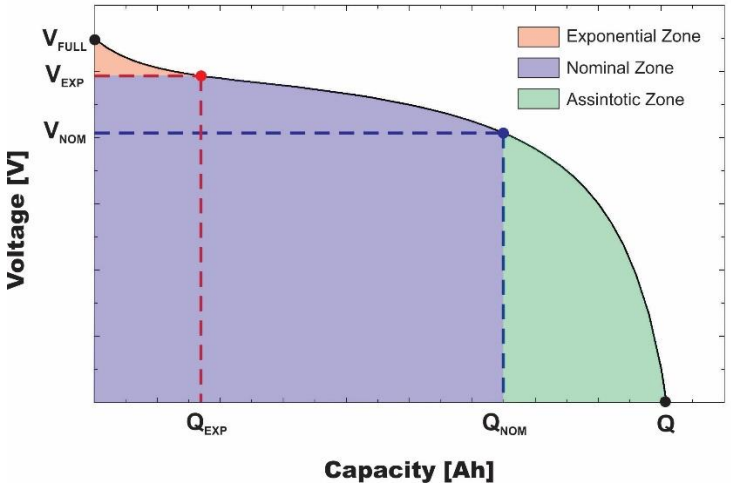

Figure 3. Battery discharge curve with time (Modified from RASZMANN, 2017)

This study considers only the operation conditions within the nominal zone, where the variation of energy with time is constant (this means the energy rate exiting the battery is constant and equal to $\dot{W}_{BAT}$), as shown by Eq. (6a). The power of the battery is given by Eq. (6b).

$$\frac{dE_{BAT}}{dt} = \dot{W}_{BAT} \quad (6a)$$

$$\dot{W}_{BAT} = V_{BAT} \cdot i \quad (6b)$$

The battery discharge behavior is described by Eq. (7) (Costa et al, 2017), for the nominal zone.

$$V_{BAT} = E_0 - K\frac{Q}{Q - i_T} - iR + Ae^{-i_T B} \quad (7)$$

E_0 is the internal tension, V_{NOM} is the tension at the end of the nominal zone, V_{FULL} full charge tension, V_{EXP} is the tension at the end of the exponential zone, K is the polarization constant, Q is maximal capacity, Q_{NOM} is nominal capacity at the end of the nominal zone, Q_{EXP} is the capacity at the end of the exponential zone, R is the internal resistance, iT is the capacity extracted, i is the charge/discharge current, A is the amplitude of the exponential zone and B is the inverse charge constant. These data are found in the manufacturer catalog. Equations (8a) to (8g) calculate these parameters.

$$E_0 = V_{FULL} + K + iR - A \tag{8a}$$

$$K = \frac{\{V_{FULL} - V_{NOM} + A[exp(-B \cdot Q_{NOM}) - 1]\} \cdot (Q - Q_{NOM})}{Q_{NOM}} \tag{8b}$$

$$Q = i_{NOM} \cdot t \tag{8c}$$

$$R = V_{NOM} \cdot \frac{1 - \eta_{BAT}}{0{,}2 \cdot Q_{NOM}} \tag{8d}$$

$$\eta_{BAT} = 1 - \frac{0{,}2 \cdot R \cdot Q_{NOM}}{V_{NOM}} \tag{8e}$$

$$A = V_{FULL} - V_{EXP} \tag{8f}$$

$$B = \frac{3}{Q_{EXP}} \tag{8g}$$

In the fuel tank, the accumulated chemical exergy ($\dot{W}_{FUE}$) decreases with time. In aeronautical applications, it is essential to model this variation, as it directly affects the weight of the aircraft and its autonomy. The exergy outlet of the tank varies with the combustion of the fuel. However, analogously to the batteries, herein the operation considers a constant energy outlet, as expressed in Eq. (9):

$$\frac{dE_{STG}}{dt} = \dot{W}_{FUE} \tag{9}$$

For the exergy analysis of the fuel, the chemical exergy, ξ, was employed. This exergy is given by the exergy:energy ratio of a specific $C_\alpha H_\gamma$ fuel, expressed by Eq. (10) (Dincer, 2013).

$$\xi = 1.0401 + 0.01728 \cdot \left(\frac{\gamma}{\alpha}\right) \tag{10}$$

Where γ is the number of hydrogen and α is the number of carbon in the chemical representation of the fuel. The exergy of the fuel ($\dot{X}^{\phi}_{FUE}$) is then given by Eq. (11) (Machado, 2019).

$$\dot{X}^{\phi}_{FUE} = \frac{\left(LHV \cdot \dot{m}^{\phi}_{FUE}\right)}{\xi} \tag{11}$$

LHV represents the lower heating value of the fuel and $\dot{m}^{\phi}_{FUE}$ is the mass flow of fuel, which depends on the ϕ. The lower the ϕ (more intense use of ICE), the higher the consumption of fuel and consequently its mass flow.

For the exergy analysis of ICE, an exergy balance was developed (according to Figure 4), resulting in Eq. (12).

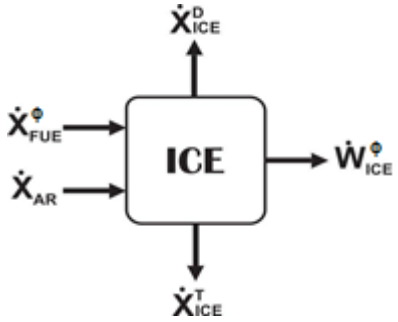

Figure 4. Exergy balance for ICE

$$\dot{X}_{AR} + \dot{X}_{FUE}^{\phi} = \dot{X}_{ICE}^{T} + \dot{W}_{ICE}^{\phi} + \dot{X}_{ICE}^{D} \quad (12)$$

$\dot{X}_{AR}$ refers to air exergy; $\dot{X}_{ICE}^{T}$ is thermal exergy in to ICE; $\dot{W}_{ICE}^{\phi}$ is power of ICE and $\dot{X}_{ICE}^{D}$ is destroyed exergy in ICE. $\dot{X}_{AR} = 0$ because the temperature and pressure conditions are the same as the environment. $\dot{X}_{ICE}^{T} = 0$ as in this case the exhaust gases are emitted to the atmosphere (wasted).

According to Çengel (2013), the transfer of exergy by work, such as electric work, is equal to the work itself. The exergies of the battery ($\dot{X}_{BAT}^{\phi}$), converters ($\dot{X}_{CON}^{\phi}$) and of the electric engine ($\dot{X}_{EME}^{\phi}$) are given by Eq. (13a), (13b) and (13c).

$$\dot{X}_{BAT}^{\phi} = \dot{W}_{BAT}^{\phi} \quad (13a)$$

$$\dot{X}_{CON}^{\phi} = \dot{W}_{CON}^{\phi} \quad (13b)$$

$$\dot{X}_{EME}^{\phi} = \dot{W}_{EME}^{\phi} \quad (13c)$$

2.3. Efficiency of components

For the converters and the propeller, modeling employed inlet/outlet power data for each subsystem. The subsystems were modeled in MatLab (Mathworks, 2020), and the corresponding outlet powers in steady state were calculated. The complex model of each subsystem was then substituted by the corresponding variable efficiency equations obtained. This simplified modeling reduces computational processing time, without decreasing precision.

Equations (14a) and (14b) were obtained empirically and are utilized for the converters – $\eta_{CON;1}$ refers to the converter connected to the ICE, and $\eta_{CON;2}$ to the converter connected to the BAT.

$$\eta_{CON;1} = 0.88 \cdot \left[1 - exp\left(-\frac{\dot{W}_{ICE}}{4000} - 0.7\right)\right] \quad (14a)$$

$$\eta_{CON;2} = 0.914 \cdot \left[1 - exp\left(-\frac{\dot{W}_{BAT}}{3900} - 0.38\right)\right] \quad (14b)$$

The efficiency of the propeller is given by Eq. (15).

$$\eta_{PRP} = 1.2384 \cdot 10^{-13} \cdot \dot{W}_{EME}{}^{3} - 6.1195 \cdot 10^{-9} \cdot \dot{W}_{EME}{}^{2} + 7.1403 \cdot 10^{-5} \cdot \dot{W}_{EME} + 0.7866 \quad (15)$$

ICE efficiency is given by Eq. (16).

$$\eta_{ICE} = 4.8424 \cdot 10^{-11} \cdot \dot{W}_{FUE}{}^{2} - 5.6016 \cdot 10^{-6} \cdot \dot{W}_{FUE} + 0.19325 \quad (16)$$

The efficiency of the battery and of the electric engine were considered constant inputs.

The distance traveled per unit quantity of energy is an important parameter, defined as the energy specific air range (ESAR) with units of meters per Joule, given by eq. (17a), (17b) and (17c) (Pornet et al., 2013 e Seitz et al, 2012).

$$ESAR = \frac{(Vel_{ACF} * L_D)}{(TSPC \cdot m_{ACF} \cdot g)} \quad (17a)$$

$$TSPC = \frac{\dot{W}_{FUE} + \dot{W}_{BAT}}{T} \quad (17b)$$

$$T = 2{,}84 \cdot 10^{-6} \cdot \dot{W}_{PRP}{}^{2} - 0{,}091 \cdot \dot{W}_{PRP} + 1124 \quad (17c)$$

TSPC is Thrust Specific Fuel Consumption, *T* is thrust, *g* is gravity, Vel_{ACF} is the flight speed and L_D is the lift-to-drag ratio.

2.4. Thermoeconomics

The thermoeconomic assessment applies the Theory of Exergy Cost (TEC) as proposed by Valero and Lozano (1993). This theory presents a series of postulates with the purpose of defining and determining the exergy cost of the final product and evaluating the global exergy efficiency. This theory includes a set of postulates to define and determine the exergy costs of the final product and evaluate the global exergy efficiency. According to Valero et al. (1992), TEC has the purpose of building a set of equations that can help solve complex energy problems that would not be solved using a conventional analysis, based on the First Law of Thermodynamics only (FLT, mass and energy balances). TEC can: i) determine the exergy costs for each flow of the hybrid system; ii) optimize specific variables of each component to minimize the costs of the final product (global and local optimization); iii) detect inefficiencies and calculate the economic repercussions (thermoeconomic diagnosis), and iv) evaluate several design alternatives or operation strategies.

Firstly, the flows between the units must be determined. The flows are exergy costs and are represented by "C", expressing the amount of exergy required to obtain each of the flows. In the study object, each subsystem presents only one exergy product with its respective cost, and the exergy flow associated with the propeller's axis is considered the main product of the analysis. The exergy cost associated with this product is C_6.

The exergy flows of the system were defined by balance equations for each component of the system, as shown in Fig. (5).

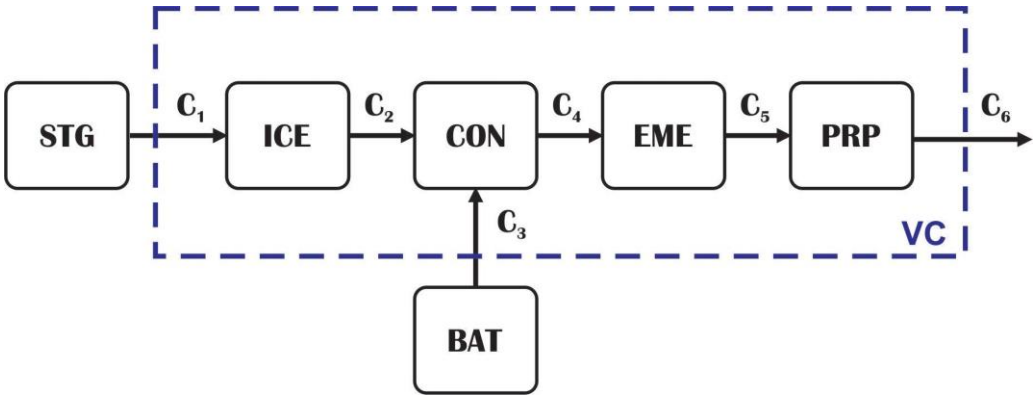

Figure 5. Exergy flows of the system

The overall cost entering the system, control volume represented by the dotted line in Fig.(4), is the sum of the exergies delivered by the fuel tank and battery throughout the trajectory analyzed. Analysis of the reservoirs is an external analysis.

The exergy cost C_1 represents the flow from the fuel tank to the ICE, defined as the exergy associated with the input of fuel to ICE and expressed by Eq. (18).

$$C_1 = \dot{X}^{\phi}_{FUE} \tag{18}$$

C_1 depends on the degree of hybridization. Exergy cost C_2 represents the exergy flow between the ICE and the converters. C_2 is defined as the exergy cost for the production of power in ICE. As this cost is associated with the fuel, C_2 is given by Eq. (19).

$$C_2 = C_1 \tag{19}$$

Exergy cost C_3 represents the flow from the batteries to the converters. It is defined as the exergy associated with the battery, and is dependent on the degree of hybridization, as shown in Eq. (20).

$$C_3 = \dot{X}^{\phi}_{BAT} \tag{20}$$

Exergy cost C_4 is the sum of the exergy costs of the fuel and battery, as shown by Eq. (21a), (21b) and (21c).

$$C_4 = C_1 + C_3 \tag{21a}$$

$$\phi = \frac{C_3}{C_1 + C_3} \tag{21b}$$

$$C_4 = \frac{C_1}{(1-\phi)} \tag{21c}$$

Exergy costs C_5 and C_6 are equal to C_4, as these flows do not receive any exergy inputs. This is expressed by Eq. (22)

$$C_5 = C_6 = C_4 \tag{22}$$

The equations can be rearranged to constitute a set of equations with the same number of equations and variables, applying the postulates of TEC, as depicted in Eq. (23) and shown in matrix form in Eq. (24).

$$\begin{cases} C_1 = \dot{X}_{FUE}^{\phi} \\ C_1 = C_2 \\ C_3 = \dot{X}_{BAT}^{\phi} \\ C_4 = \frac{C_1}{(1-\phi)} \\ C_5 = C_4 \\ C_6 = C_5 \end{cases} \tag{23}$$

$$\begin{matrix} C_1 & C_2 & C_3 & C_4 & C_5 & C_6 \end{matrix}$$
$$\begin{bmatrix} 1 & 0 & 0 & 0 & 0 & 0 \\ 1 & -1 & 0 & 0 & 0 & 0 \\ 0 & 0 & 1 & 0 & 0 & 0 \\ 1 & 0 & 0 & (1-\phi) & 0 & 0 \\ 0 & 0 & 0 & 1 & -1 & 0 \\ 0 & 0 & 0 & 0 & 1 & -1 \end{bmatrix} = \begin{bmatrix} \dot{X}_{FUE}^{\phi} \\ 0 \\ \dot{X}_{BAT}^{\phi} \\ 0 \\ 0 \\ 0 \end{bmatrix} \tag{24}$$

2.5. Simulations

The mathematical models were implemented in the Engineering Equation Solver (EES, 2020). The parametric analysis was carried out by varying the ϕ between 0 and 1.

Table 1 – Input data for the simulations.

Battery efficiency	η_{BAT}	0.95
Electric engine efficiency	η_{EME}	0.9661
Flight speed of aircraft	Vel_{ACF}	37.3 [m/s]
Drag coefficient of the aircraft	L_D	12.5
Maximum power of fuel	$\dot{W}_{FUE;max}$	126000 [W]
Minimal fuel energy rate	$\dot{W}_{FUE;min}$	42000 [W]
Lower heating value of the fuel	LHV	42580 [kJ/kg]
Exergy-energy relationship of the fuel	ξ	1.073
Battery capacity at the end of exponential zone	Q_{EXP}	8 [Ah]
Battery capacity at the end of nominal zone	Q_{NOM}	32 [Ah]
Nominal capacity of battery	Q	40 [Ah]
Internal resistance of battery	R	0.0007 [Ω]
Full charge tension	E_{FULL}	3.35 [V]
Battery tension at the end of exponential zone	E_{EXP}	3.3 [V]
Battery tension at the end of nominal zone	E_{NOM}	3.1 [V]
Nominal current of battery	i	20 [A]

The parameters selected for the analysis were: the variation of the battery energy output rate ($\dot{W}_{BAT}$), output power at propeller ($\dot{W}_{PRP}$), thrust generated by the propeller (T), relationship power/thrust (thrust specific power consumption, *TSPC*), efficiency of ICE (η_{ICE}), efficiency of propeller (η_{PRP}), energy specific air range (*ESAR*) and the exergy cost of the output (C_6). Table 1 shows the input data.

3. RESULTS

The following curves were plotted for the selected parameters in function of ϕ, which varied between *0* (only ICE) and *1* (battery propulsion).

Figure 6 shows the variation of the battery energy output (W_{BAT}), over the duration of the analyzed flight plan, varying with the degree of hybridization (ϕ). It can be seen that the curves have a tendency similar to the battery discharge curve as the literature proposes. It is also observed that the W_{BAT} has higher values for greater values of ϕ.

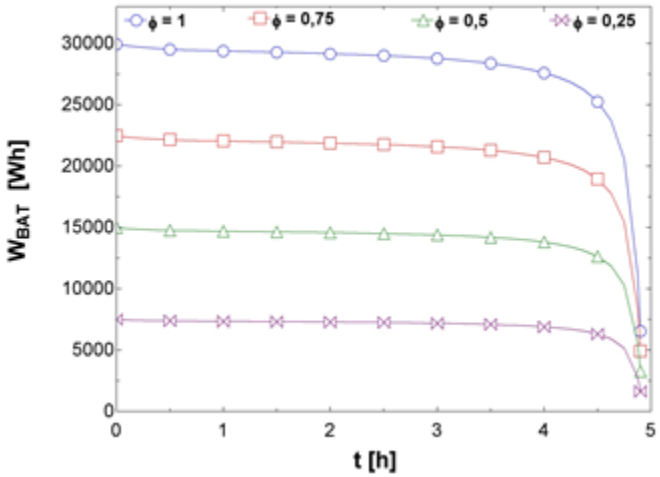

Figure 6. Variation of the battery's energy output in function of the degree of hybridization and flight time

Figure 7 shows how the output power of the propeller varies with ϕ. The minimal value $\dot{W}_{PRP}$ = 14214 W is obtained for ϕ = 0.42.

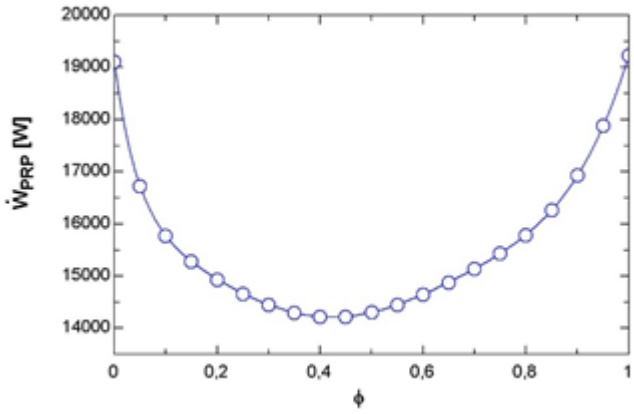

Figure 7. Output power of propeller in function of the degree of hybridization (ϕ)

Figure 8 shows how the thrust (T) generated by the propeller varies with ϕ. Minimal values T = 395 N are obtained at two points, ϕ = 0.08 and ϕ = 0.84. Between these two minima. there is a maximal point at T = 404N with ϕ = 0.42. This maximal point occurs exactly where the propeller's power is minimal - as the efficiency of the propeller is maximal at this point, it generates higher thrust with lower power.

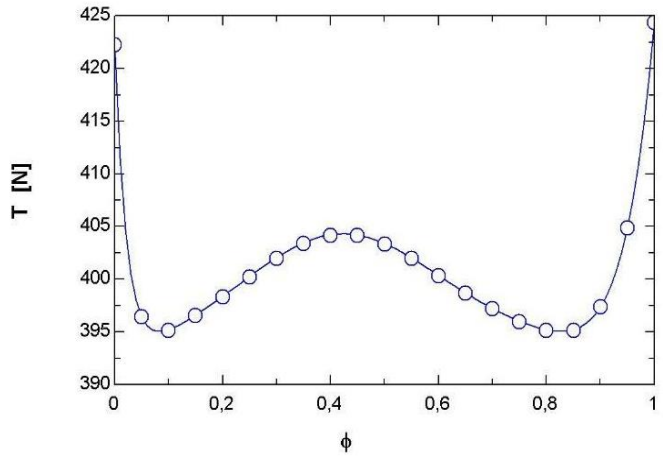

Figure 8. Thrust generated by the propeller in function of the degree of hybridization (ϕ)

Figure 9 shows the relationship between power/thrust in function of ϕ. It can be observed that the curve peaks at *TSPC* = 311 W/N for ϕ = 0.04. After this value, the graph decreases at an almost constant rate. This happens because at the central point (maximal thrust), the sum of power inlets (W_{ICE} and W_{BAT}) is minimal.

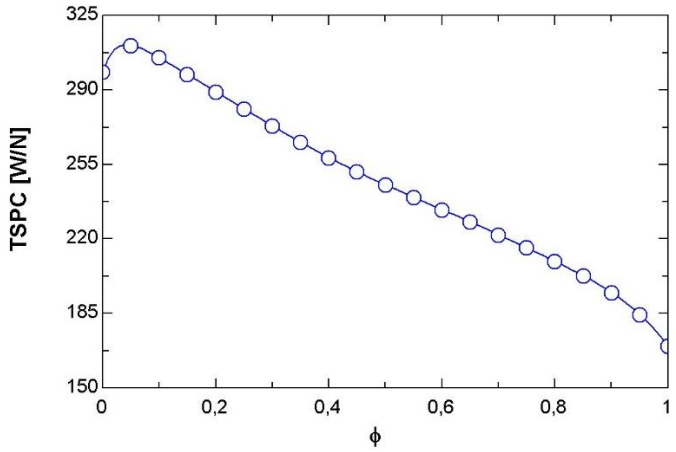

Figure 9. Power/thrust ratio vs. degree of hybridization (ϕ).

Figure 10 shows the variation of the ICE efficiency vs. ϕ. It is possible to notice that the curve reaches a minimal at η_{ICE} = 0.03 and ϕ = 0.81. This behavior was expected, as the maximal efficiency of ICE occurs at full load, i.e., ϕ = 0.

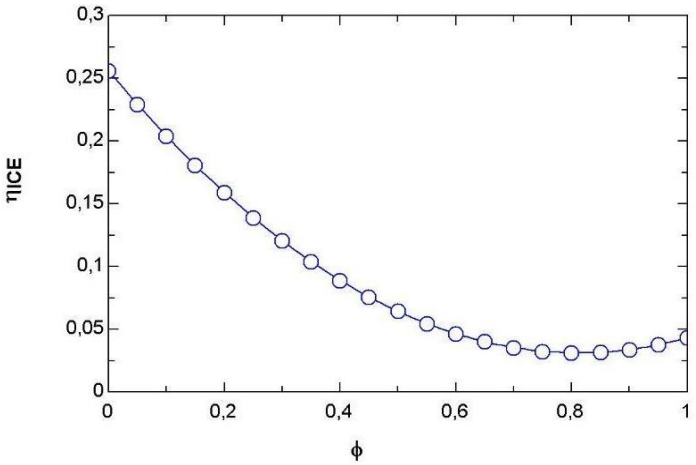

Figure 10. Efficiency of ICE vs. degree of hybridization

Figure 11 depicts the variation of propeller efficiency vs. ϕ. The curve reaches a maximal value at η_{PRP} = 0.84 and ϕ = 0.43. This curve presents an inverse behavior to the thrust curve, as the thrust generated by the propeller depends directly on its efficiency.

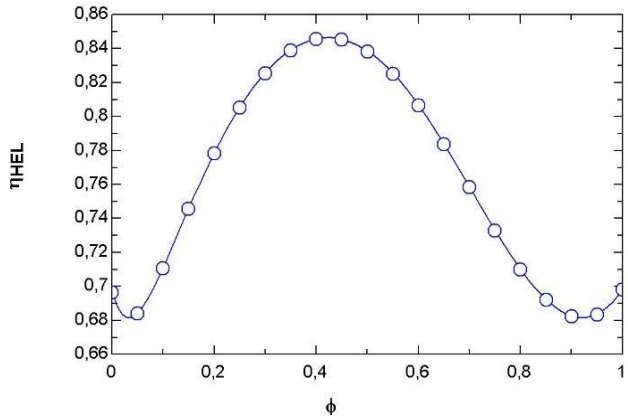

Figure 11. Propeller efficiency vs. degree of hybridization

Figure 12 shows the variation of *ESAR* with respect to ϕ. The curve presents an increasing behavior, almost linear. This occurs because of two factors: i) the weight of the battery is fixed (its weight does not change with the distance travelled) and the fossil fuel is burned and eliminated in the form of exhaust gases as distance is travelled, and ii) for higher ϕ values, the value of the power/thrust ratio decreases.

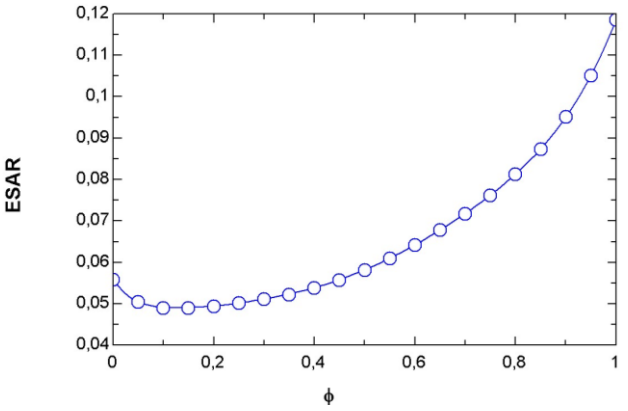

Figure 12. Energy specific air range (ESAR) *vs.* ϕ

Figure 13 shows the variation of the final exergy cost vs. ϕ. The exergy cost increases exponentially as the degree of hybridization reaches 1. This demonstrates that the exergy cost of a purely electric aircraft (ϕ = 1) is higher than the exergy cost of a conventional aircraft (ϕ = 0).

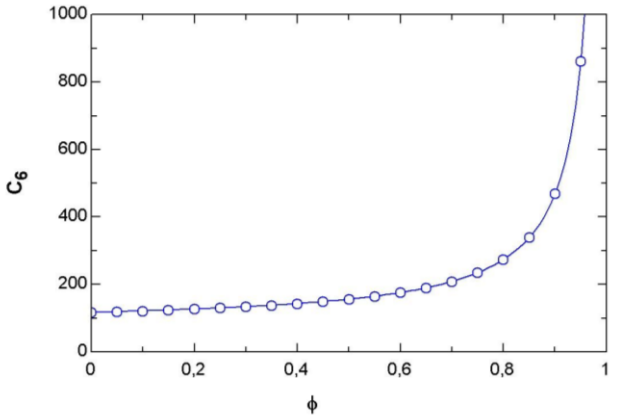

Figure 13. Final exergy cost vs. degree of hybridization

Hybrid-electric propulsion is becoming an interesting alternative for the aviation sector, taking advantage of the synergy between two technologies by utilizing both ICE and electric motors together, each operating at their respective optimum conditions. As mentioned by Aigner et al. (2018), hybrid electric propulsion concepts are scalable with regard to flight range and payload and are considered to achieve similar operational flexibility as current conventional technologies - hybrid electric propulsion technologies have been in the research spotlight regarding preliminary aircraft design research projects in recent years.

Due to recent concerns on fossil fuel reserves, carbon emissions, noise pollution, and stricter regulations on safety and performance, hybrid-electric propulsion can be part of a sustainable pathway. The COVID-19 crisis has added turmoil to the global energy system, causing serious disruptions in electric systems (Carvalho et al., 2020) and slowing down (but not halting) the energy transition. Energy efficiency schemes can include hybrid-electric propulsion, and research should focus on new aerodynamic concepts, propulsion components and their impact in the overall transportation system.

4. CONCLUSIONS

Hybrid-electric propulsion is an excellent candidate for the aeronautical sector, taking advantage of the synergy between two technologies by combining the complementary advantages of internal combustion and electric propulsion technologies while limiting environmental emissions. Within this contribution, a hybrid-electric system was modeled from power, exergy, and efficiency equations for each component. From these equations, it was possible to simulate the energy and exergy behavior of the system for maximum propulsion, varying the degree of hybridization (ϕ).

Regarding the output power of the propeller, the minimal value of 14214 W is obtained for $\phi = 0.42$. When thrust was analyzed, two minimal values of 395 N were found, at $\phi = 0.08$ and $\phi = 0.84$. Between these two minima. there is a maximal point with 404 N and $\phi = 0.42$.

When the relationship between power and thrust in function of ϕ was analyzed, the curve peaks at Thrust Specific Fuel Consumption = 311 W/N for $\phi = 0.04$. After this value, the graph decreases at an almost constant rate. Regarding ICE efficiency vs. ϕ, the curve reaches a minimal at $\eta_{ICE} = 0.03$ and $\phi = 0.81$.

For the energy specific air range (*ESAR*) *vs.* ϕ, the curve presents an almost linear, increasing behavior. When the final exergy cost was varied along with ϕ, the exergy cost also presented an upwards behavior, increasing exponentially as the degree of hybridization reaches 1.

Hybrid-electric configurations show promising complementarities to internal combustion engine-only propulsive configurations, and future directions of research can include battery charge cycles that enable downsizing the internal combustion engine.

5. ACKNOWLEDGMENTS

The authors wish to thank UFJF and FAPEMIG for the support provided to carry out this study. Thanks are extended to the Board of Technological Development of EMBRAER, for the partnership that enabled the advance in technical-scientific knowledge. The authors also wish to acknowledge the support of the National Council for Scientific and Technological Development (CNPq, Brazil) Research Productivity grant nº 307394/2018-2.

6. REFERENCES

Affonso, W., Gandolfi, R., da Silva, R. G., & Junior, S. D. (2019). Exergy and Exergoeconomic Comparative Analysis Between Conventional and Hybrid Electric Propulsion Systems for a Regional Aircraft. In AIAA Aviation 2019 Forum (p. 3682).

Aigner, B., Nollmann, M., & Stumpf, E. (2018). Design of a hybrid electric propulsion system within a preliminary aircraft design software environment. In Deutscher Luft-und Raumfahrtkongress.

Benito, Y., "Modelagem da produção simultânea de frio, calor e energia elétrica", PUC-Rio, Rio de Janeiro, 2007

Carvalho, M., de Delgado, D. B., de Lima, K. M., de Cancela, M., dos Siqueira, C. A., & de Souza, D. L. B. (2020). Effects of the COVID-19 pandemic on the Brazilian electricity consumption patterns. International Journal of Energy Research, e5877.

Çengel, Y.A.; Boles, M.A. Thermodynamics: An Engineering Approach. 8ª ed. São Paulo: Editora McGraw-Hill, 2014.

Dincer, I.; Rosen, M.A. Exergy: Energy, Environment and Sustainable Development. 2nd edition. Elsevier Ltd, 2013.

Finger, D. F., Götten, F., Braun, C., & Bil, C. (2018, October). On aircraft design under the consideration of hybrid-electric propulsion systems. In Asia-Pacific International Symposium on Aerospace Technology (pp. 1261-1272). Springer, Singapore.

Friedrich, C., & Robertson, P. A. (2015). Hybrid-electric propulsion for aircraft. Journal of Aircraft, 52(1), 176-189.

Gandolfi, R., Pellegrini, L., & de Oliveira, S. (2010). More electric aircraft analysis using exergy as a design comparison tool. In 48th AIAA Aerospace Sciences Meeting Including the New Horizons Forum and Aerospace Exposition (p. 809).

Hoelzen, J., Liu, Y., Bensmann, B., Winnefeld, C., Elham, A., Friedrichs, J., & Hanke-Rauschenbach, R. (2018). Conceptual design of operation strategies for hybrid electric aircraft. Energies, 11(1), 217.

Koruyucu, E. (2019). Energy and exergy analysis at different hybridization factors for hybrid electric propulsion light utility helicopter engine. Energy, 189, 116105.

Engineering Equation Solver. (2020). F-chart software. Available at: <http://www.fchartsoftware.com/ees/> Accessed 22 jul 2020.

Machado, G.S. Análise Termoeconômica da Propulsão Híbrido-Elétrica em Aeronaves (Estudo De Caso). 64 p. Universidade Federal de Juiz de Fora. Juiz de Fora. MG. 2019

Mathworks. MatLAB. (2020a) Available at <https://www.mathworks.com/products/matlab.html> Accessed 29 jul 2020.

Pornet, C. Methodology for Sizing and Performance Assessment of Hybrid Energy Aircraft. Journal Of Aircraft: Aerospace Research central. Los Angeles Ca, p. 1-12. 29 abr. 2013.

Seitz, A., Schmitz, O., Isikveren, A. T., and Hornung, M., "Electrically Powered Propulsion: Comparison and Contrast to Gas Turbines," Deutscher Luft- und Raumfahrt Kongress, DLRK, Berlin, 2012.

Sziroczak, D., Jankovics, I., Gal, I., & Rohacs, D. (2020). Conceptual design of small aircraft with hybrid-electric propulsion systems. Energy, 117937.

Song, K., Liu, L., Li, F., & Feng, C. (2019, September). Degree of Hybridization Design for a Fuel Cell/Battery Hybrid Electric Vehicle Based on Multi-objective Particle Swarm Optimization. In 2019 3rd Conference on Vehicle Control and Intelligence (CVCI) (pp. 1-6). IEEE.

Valero, A. Lozano, M. A. Theory of the Exergetic Cost, Energy, Vol 1, No 9, pp. 939-960. 1993.

Valero A., L. Serra, and C. Torres (1992). A General Theory of Thermoeconomics: Part I: Structural Analysis. International Symposium ECOS'92. ASME Book I00331, 137-145. Zaragoza, Spain.

7. RESPONSIBILITY NOTICE

The authors are the only responsible for the printed material included in this paper.